Eur. Phys. J. B **25**, 89–100 (2002)
DOI: 10.1140/e10051-002-0010-1

THE EUROPEAN PHYSICAL JOURNAL B
EDP Sciences

Scattering of vortex pairs in 2D easy-plane ferromagnets

A.S. Kovalev[1], S. Komineas[2,a], and F.G. Mertens[2]

[1] Institute for Low Temperature Physics and Engineering, 47 Lenin Ave., 61164 Kharkov, Ukraine
[2] Physikalisches Institut, Universität Bayreuth, 95440 Bayreuth, Germany

Received 18 September 2001

Abstract. Vortex-antivortex pairs in 2D easy-plane ferromagnets have characteristics of solitons in two dimensions. We investigate numerically and analytically the dynamics of such vortex pairs. In particular we simulate numerically the head-on collision of two pairs with different velocities for a wide range of the total linear momentum of the system. If the momentum difference of the two pairs is small, the vortices exchange partners, scatter at an angle depending on this difference, and form two new identical pairs. If it is large, the pairs pass through each other without losing their identity. We also study head-tail collisions. Two identical pairs moving in the same direction are bound into a moving quadrupole in which the two vortices as well as the two antivortices rotate around each other. We study the scattering processes also analytically in the frame of a collective variable theory, where the equations of motion for a system of four vortices constitute an integrable system. The features of the different collision scenarios are fully reproduced by the theory. We finally compare some aspects of the present soliton scattering with the corresponding situation in one dimension.

PACS. 75.10.Hk Classical spin models – 75.70.Kw Domain structure (including magnetic bubbles) – 05.45.Yv Solitons

1 Introduction

The statics and dynamics of magnetic vortices is already an old subject [1–4]. An increasing interest in the problem has arisen again [5–7] which is connected with the synthesis and experimental study of new low-dimensional magnetic compounds such as two-dimensional magnetic lipid layers, organic intercalated quasi-2D layered magnets and HTSC-materials in the antiferromagnetic state.

Magnetic vortices play an important role in easy-plane magnets. They are the main ingredients in the Kosterlitz-Thouless phase transition. At a finite temperature the density of vortices is large and they should give a considerable contribution to the dynamic correlations.

We already have a detailed picture of the dynamics in a system with a small number of vortices. An isolated vortex in an infinite system can only move together with the background flux [3,8]. Two vortices interact and undergo Kelvin motion if they have opposite topological charges while they move one around the other when they have the same charge. We shall call the pair of two vortices with opposite topological charge a vortex-antivortex pair (V-A pair). Such pairs can have the characteristics of a soliton in the sense that they move coherently with some constant velocity. Solitons of this kind have been numerically investigated in some magnetic systems [9,10]. Analogous V-A pairs have been studied in superfluids [11–13], nonlinear optics [14] and hydrodynamics [15].

In a system with a lot of vortices the picture becomes accordingly more complicated. If we suppose a dilute vortex gas, the average velocity is $\overline{V} \sim \sqrt{\rho} \sim 1/L$, where ρ is the density of vortices and L the average distance between them. The interaction energy is proportional to the logarithm of the average distance. This picture should be realistic above the Kosterlitz-Thouless temperature. At low temperatures vortex-antivortex pairs are expected to form. The energy of a pair is finite and it is proportional to the logarithm of its size. The interaction potential between them is inversely proportional to the second power of their size. One may be tempted to treat the vortex pairs as elementary weakly interacting particles. However, their dynamics is not Newtonian and most importantly they have an internal structure which may change during interaction.

In a dense enough gas of vortices, interactions among traveling V-A pairs are unavoidable. In particular, any change in the number of vortices present in the system, or the number of vortices in equilibrium, should be a direct or indirect result of the scattering among V-A pairs. Our article is devoted to head-on and head-tail collisions between V-A pairs in easy-axis ferromagnets, *i.e.* to the case of zero total angular momentum of the system. Our study is both numerical and analytical. A collective coordinate theory is found to be particularly successful and provides the basis for a clear picture of the dynamics.

[a] e-mail: stavros.komineas@uni-bayreuth.de

Our results should also be relevant for a variety of other systems where V-A pairs have been found. Furthermore comparisons can be made to the well-studied soliton interactions in one space dimension.

The outline of the rest of the paper is as follows. In Section 2 we give a short description of the system and an account of the dynamics of vortices and vortex-antivortex pairs. In Section 3 we present numerical simulations for collisions between V-A pairs. Section 4 presents a theory which explains the features of the dynamical behavior of vortex pairs. Our concluding remarks are contained in the last Section 5.

2 Vortices and vortex-antivortex pairs

We consider the classical two-dimensional Heisenberg ferromagnet with a uniaxial anisotropy of the easy-plane type. The corresponding Hamiltonian has the form

$$\mathcal{H} = -J \sum_{(n,m)} (\mathbf{S}_n \cdot \mathbf{S}_m) + \frac{\beta}{2} \sum_n (S_n^z)^2, \tag{1}$$

where $\mathbf{S}_n$ denotes the spin variable at site n, S_n^z is the third component of $\mathbf{S}_n$. The first summation runs over the nearest-neighbor pairs. The exchange constant J and the single-ion anisotropy constant β are positive. We treat the spin $\mathbf{S}$ as a classical vector of constant length. Usually the magnetic anisotropy is small: $\beta/J \sim 10^{-2}$ or 10^{-3}. In this case we can use a continuum approximation of the Hamiltonian. We define two fields $m = S^z$ and $\Phi = \arctan(S^y/S^x)$, where S^x, S^y, S^z are the Cartesian components of the spin. In terms of these variables the continuum version of the Hamiltonian reads

$$\mathcal{H} = \frac{\beta}{2} \int \mathrm{d}x\mathrm{d}y \left[\frac{(\nabla m)^2}{1-m^2} + (1-m^2)\,(\nabla \Phi)^2 + m^2 \right]. \tag{2}$$

The coordinates x, y are measured in units of the "magnetic length" $l_0 = \sqrt{J/\beta}$. m, Φ are canonically conjugate fields and the equations of motion have the Hamiltonian form [17]

$$\frac{\partial \Phi}{\partial t} = \frac{\delta \mathcal{H}}{\delta m}, \qquad \frac{\partial m}{\partial t} = -\frac{\delta \mathcal{H}}{\delta \Phi}, \tag{3}$$

explicitly

$$\frac{\partial \Phi}{\partial t} = m - \frac{\Delta m}{1-m^2} - \frac{m\,(\nabla m)^2}{(1-m^2)^2} - m\,(\nabla \Phi)^2,$$

$$\frac{\partial m}{\partial t} = (1-m^2)\,\Delta \Phi - 2\,m\,\nabla m \nabla \Phi. \tag{4}$$

Our numerical algorithm uses the formulation through the stereographic variable

$$\Omega = \sqrt{\frac{1-m}{1+m}}\ \exp(\mathrm{i}\Phi). \tag{5}$$

This satisfies the equation

$$\mathrm{i}\,\frac{\partial \Omega}{\partial t} = -\Delta \Omega + \frac{2\,\overline{\Omega}}{1+\Omega\overline{\Omega}}\,\partial_\mu \Omega\,\partial_\mu \Omega - \frac{1-\Omega\overline{\Omega}}{1+\Omega\overline{\Omega}}\,\Omega, \tag{6}$$

where $\overline{\Omega}$ denotes the complex conjugate of Ω. This variable was used in the solution of the Landau-Lifshitz equation in one dimension since, in terms of it, the soliton solutions attain their simplest form [17,18].

In studying statics and dynamics for the above model, the topological density

$$\gamma = \frac{\partial m}{\partial x}\frac{\partial \Phi}{\partial y} - \frac{\partial m}{\partial y}\frac{\partial \Phi}{\partial x} \tag{7}$$

is a most useful quantity. It has been called the "local vorticity" since it plays here a role analogous to the ordinary vorticity in fluid dynamics [8,19]. The integrated topological density

$$\Gamma = \int \gamma\,\mathrm{d}x\mathrm{d}y \tag{8}$$

is an invariant and takes values which are integral multiples of 2π for the vortex solutions that we shall discuss here.

The vorticity density enters the definitions of the linear and angular momentum of the theory which read [8]

$$P_\mu = -\varepsilon_{\mu\nu} \int x_\nu\,\gamma\,\mathrm{d}x\mathrm{d}y, \quad \mu,\nu = 1,2, \tag{9}$$

$$\ell = \int (x^2+y^2)\,\gamma\,\mathrm{d}x\mathrm{d}y. \tag{10}$$

The role of the total vorticity in the dynamics can be also appreciated through the definition of the so-called "gyrocoupling vector" [20]

$$\mathbf{G} = -\hat{\mathbf{z}}\,\Gamma, \tag{11}$$

where $\hat{\mathbf{z}}$ is the unit vector in the third direction. The gyrocoupling vector enters the equations which describe the dynamics of vortices in a collective coordinate theory.

We now turn our attention to the discussion of topological excitations. We take as a boundary condition that the field Φ is proportional to the polar angle ϕ at spatial infinity. We then obtain vortex solutions which have the form [2,3,5]

$$\Phi = \kappa\ \arctan\frac{y-Y}{x-X}, \tag{12}$$

$$m = f(|\mathbf{r}-\mathbf{R}|), \tag{13}$$

where $\kappa = \pm 1, \pm 2, \ldots$ will be called the vortex number and (X,Y) is the position of the vortex center. In the following we call the vortices with $\kappa < 0$ antivortices. The magnetization field m for a vortex can be found numerically and has the following asymptotic behavior [5]:

$$m = \lambda\,[1 - a\,r^2], \quad r \to 0,$$

$$m = \lambda\,b\ \exp(-r)/\sqrt{r}, \quad r \gg 1, \tag{14}$$

where r is the distance from the vortex center, a, b are constants and $\lambda = m(r=0) = \pm 1$ we call the "polarity" of the vortex. The radius of the vortex is unity in our units. We use in our numerical simulations only vortices and antivortices with $\kappa = \pm 1$ and polarity $\lambda = 1$.

The total vorticity of the vortices (12, 13) is $\Gamma = -2\pi\kappa\lambda$. The structure of the magnetic vortices (12, 13) is similar to that of the vortices in a non-ideal Bose gas [11] where the quantity $(1-m)$ is the density of the Bose particles. However, the ferromagnetic vortices differ in that they come with two possible values of the polarity λ.

The most impressive characteristic of the dynamics of an isolated vortex is that it is spontaneously pinned in an infinite medium. One can trace the reasons of this dynamical behavior to their topological complexity which is reflected in the nonzero value of Γ [8]. On the other hand, a vortex-antivortex pair undergoes Kelvin motion. This motion was studied in [21,22] (see also [23]) for a large vortex separation. In general, Kelvin motion sets in when the two vortices have opposite total vorticities: $\kappa_1\lambda_1 = -\kappa_2\lambda_2$.

One can argue that the simplest topologically nontrivial objects which can be found in free translational motion should have the form of a vortex-antivortex pair with $\Gamma = 0$. A conclusive numerical and analytical study in an easy-plane ferromagnet was given in [9] where the profiles of coherently moving structures were numerically calculated. There is a branch of solitons with velocities varying from zero to unity, which is the velocity of spin waves in the medium in our units. For small velocities the solitons have indeed the form of a V-A pair with a large separation L between the vortex and the antivortex. Their velocity is inversely proportional to the distance between them

$$v = \frac{1}{L}, \qquad L \gg 1. \tag{15}$$

When the velocity approaches that of spin waves in the medium the vortex-antivortex character of the soliton is lost. The transition occurs at $v \simeq 0.78$ in the sense that above this velocity the spin does not reach the north pole at any point.

Similar ideas have a long history in hydrodynamics where V-A pairs have been studied theoretically and experimentally in 2D flows. It is known that a V-A pair undergoes Kelvin motion in a direction perpendicular to the line connecting the centers of the vortex and the antivortex and the velocity is inversely proportional to the distance between them [15,16]. However, all the studies were made in the limit of point vortices, that is all moving objects had a clear vortex-antivortex character. We shall go beyond this situation in the present paper.

3 Collisions of vortex-antivortex pairs: numerical simulations

The investigation of the interactions among the traveling V-A pairs comes as a natural next step after the well established theories of the previous section. In the following, we approach the subject through numerical simulations. We simulate collisions of pairs which are initially moving along the same line, say the horizontal x-axis. We are interested both in head-on collisions, where the pairs move initially in opposite directions and in head-tail collisions, that is when they move in the same direction.

In the first set of our simulations, we confine ourselves to V-A pairs with small velocities so that the topological characteristics remain distinct and the vortices in the pair retain their identity. In particular, the distance between the vortex and antivortex centers is larger than the size of a single vortex ($L > 1$ in our conventions). When the sizes of the simulated pairs are large, that is the distance between the vortex and the antivortex is large ($L \gg 1$), we use as an initial condition the ansatz

$$\Omega = \prod_{i=1}^{4} \Omega_i, \qquad \Omega_i = \sqrt{\frac{1-f_i}{1+f_i}}\, \mathrm{e}^{\mathrm{i}\Phi_i}, \tag{16}$$

where f_i and Φ_i are the functions in equations (12, 13). They represent vortices which are centered at $\mathbf{R_i} = (X_i, Y_i)$ and have vortex numbers κ_i. In particular we choose $\kappa_1 = -\kappa_2$, $X_1 = X_2 \equiv x_1$, $Y_1 = -Y_2 \equiv y_1$ for the first pair which has a size $L_1 = 2y_1$. We take accordingly $\kappa_3 = -\kappa_4$, and $X_3 = X_4 \equiv x_2$, $Y_3 = -Y_4 \equiv y_2$ for the second pair which has a size $L_2 = 2y_2$ (we suppose $y_1, y_2 > 0$). The above ansatz represents two V-A pairs which are moving on the x-axis and are set in a collision course, as long as the size of each pair is smaller than the distance between them: $L_1, L_2 \ll \delta \equiv |x_1 - x_2|$. As an alternative to the ansatz (16) we also use the product ansatz of two V-A pair solitons of reference [9]. This ansatz resembles in its gross features the ansatz (16).

We perform the numerical simulations on a 500×500 mesh with a uniform lattice spacing, typically $h = 0.2$. The time integration is performed by a fourth order Runge-Kutta routine.

In [24] one of the present authors has investigated the interaction process of two identical V-A pairs which collide head-on. It was found that during the collision the vortices exchange their partners and two new pairs are formed which are scattered at right angles. The trajectories of the magnetic vortices are similar to those in collisions of V-A pairs in hydrodynamics [15,16] and they conform to a good accuracy to the formula $1/X_i^2 + 1/Y_i^2 = \text{const.}$ obtained in the 19th century [25,26].

Here, we consider collisions of two V-A pairs with different velocities and consequently with different sizes. The results of our numerical simulations are summarized in Figures 1, 2, 3 and 4. Figure 1 presents head-on collisions and Figure 3 head-tail collisions through contour plots of the field $m(x, y)$ at six snapshots during the collision process. Figures 2 and 4 present the corresponding orbits of the individual vortices during the interaction process. We have traced the center of every vortex which was considered to be at the point where the field $m = 1$. The result of each process depends essentially on the difference between the sizes of the two V-A pairs. For head-on collisions we use $\kappa_1 = \kappa_4 = 1, \kappa_2 = \kappa_3 = -1$ and for head-tail collisions we use $\kappa_1 = \kappa_3 = 1, \kappa_2 = \kappa_4 = -1$.

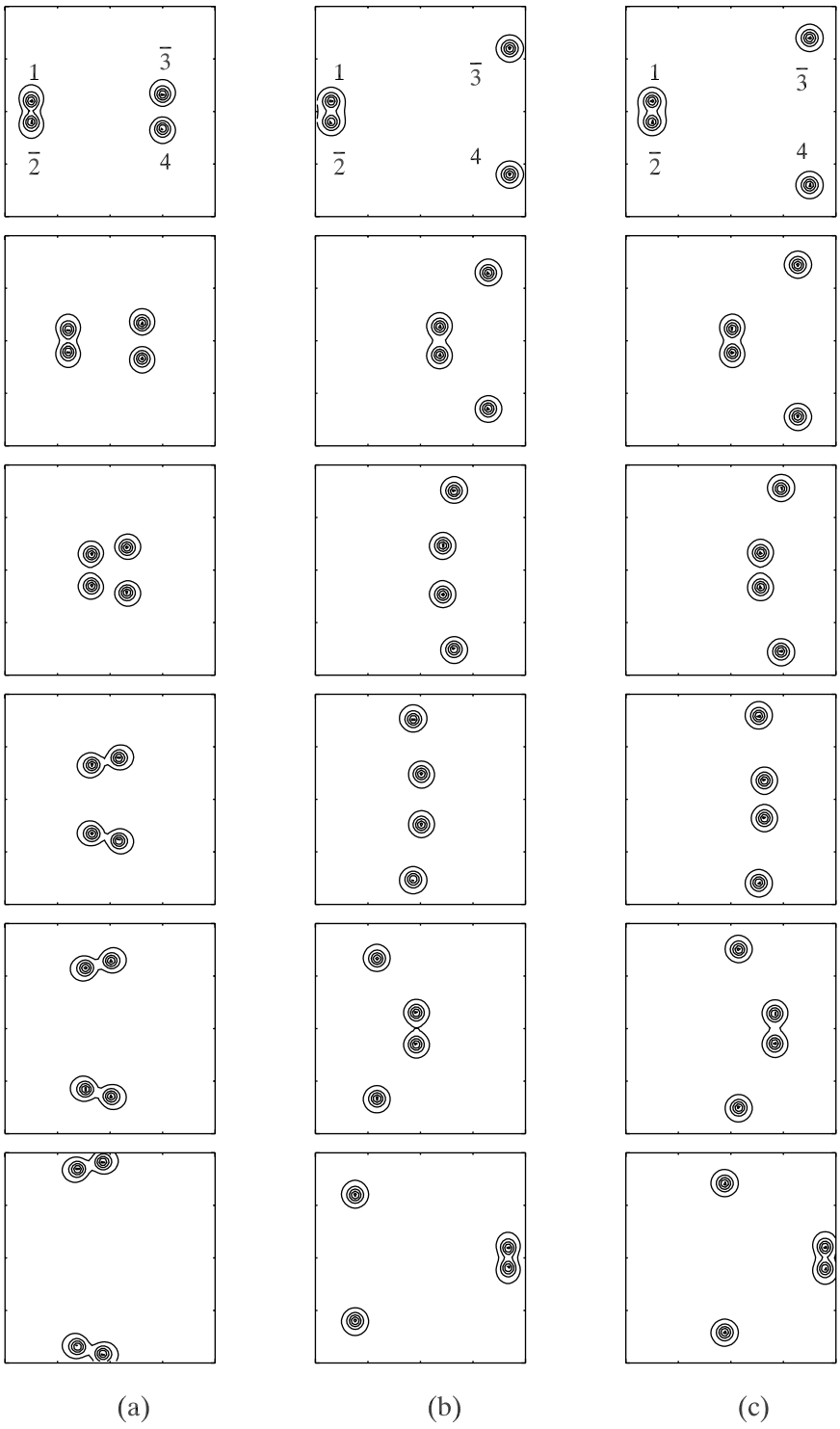

Fig. 1. Head-on collisions between vortex-antivortex pairs. We plot here contours of the third component of the spin using the levels 0.1, 0.3, 0.5, 0.7, 0.9. The numbers 1, 4 denote the vortices and the $\overline{2}$, $\overline{3}$ the antivortices. In (a) we have the case of a small difference between the linear momentum of the two pairs and the vortices exchange partners and scatter at an angle. In (b) the difference in momentum is larger. The pairs exchange partners, follow a looping orbit and finally rejoin the initial partners and travel along the initial direction of motion. In (c) the momentum difference is large. The two pairs pass through each other. Note that the boxes presented here have dimensions 40×40 while the simulations were done in a space 100×100.

Figure 1a presents the head-on collision of two pairs with a small difference between their sizes. We use here the V-A pair solitons which have been numerically calculated in [9]. The initial ansatz in our simulation is the product ansatz of two such pairs. We have taken the size of the left pair $L_1 \simeq 4$ which corresponds to a velocity $v_1 = 0.27$ and the size of the pair on the right $L_2 \simeq 6.3$ which corresponds to $v_2 = 0.15$. The initial separation measured on the x-axis is $\delta = 25$. In the scattering process the vortices exchange their partners and two new identical pairs are formed which are scattered at an angle. Varying the sizes L_1, L_2 we observe that the angle tends to 90° as the difference in the velocities (and momentums) of the two pairs is getting smaller. This process generalizes the 90° scattering of two identical solitons [24].

According to (9), the larger soliton (pair on the right) has also a larger linear momentum. Conservation of the total momentum implies that each of the resulting

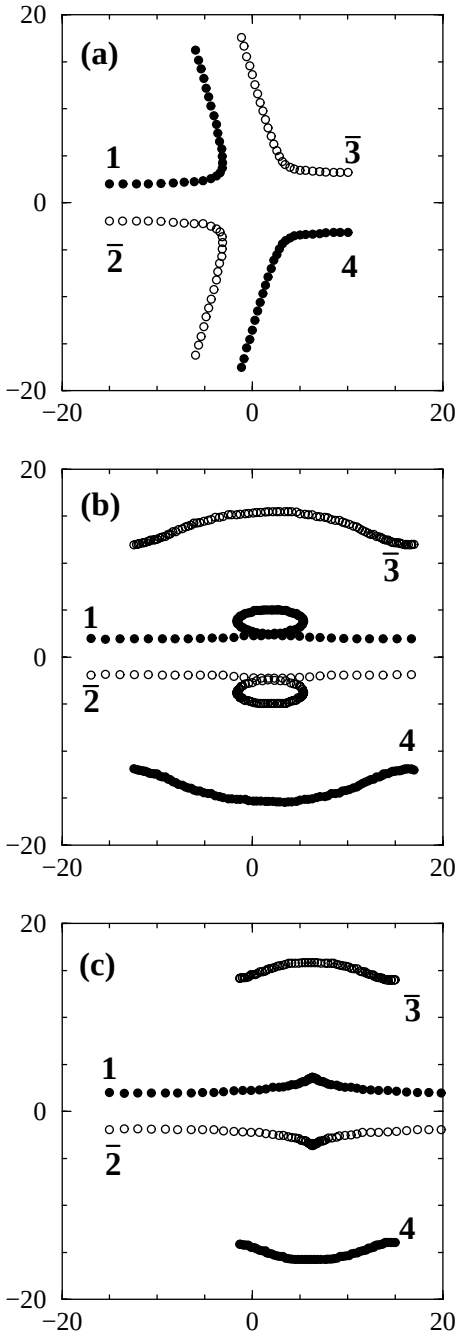

Fig. 2. The orbits of the vortices and antivortices of Figure 1 during their head-on collision. The filled circles denote the position of vortices and the open circles the position of the antivortices at successive and equal times intervals. The numbers 1, $\overline{2}$, $\overline{3}$, 4 denote the initial position of the vortices and antivortices.

identical pairs has a non-zero x-component of the momentum and a velocity to the left. Figure 2a shows the trajectories followed by each vortex and antivortex. Open circles denote the centers of the antivortices and filled circles those of the vortices.

We defer for later the case of an intermediate difference between the sizes of the two pairs and discuss first the case

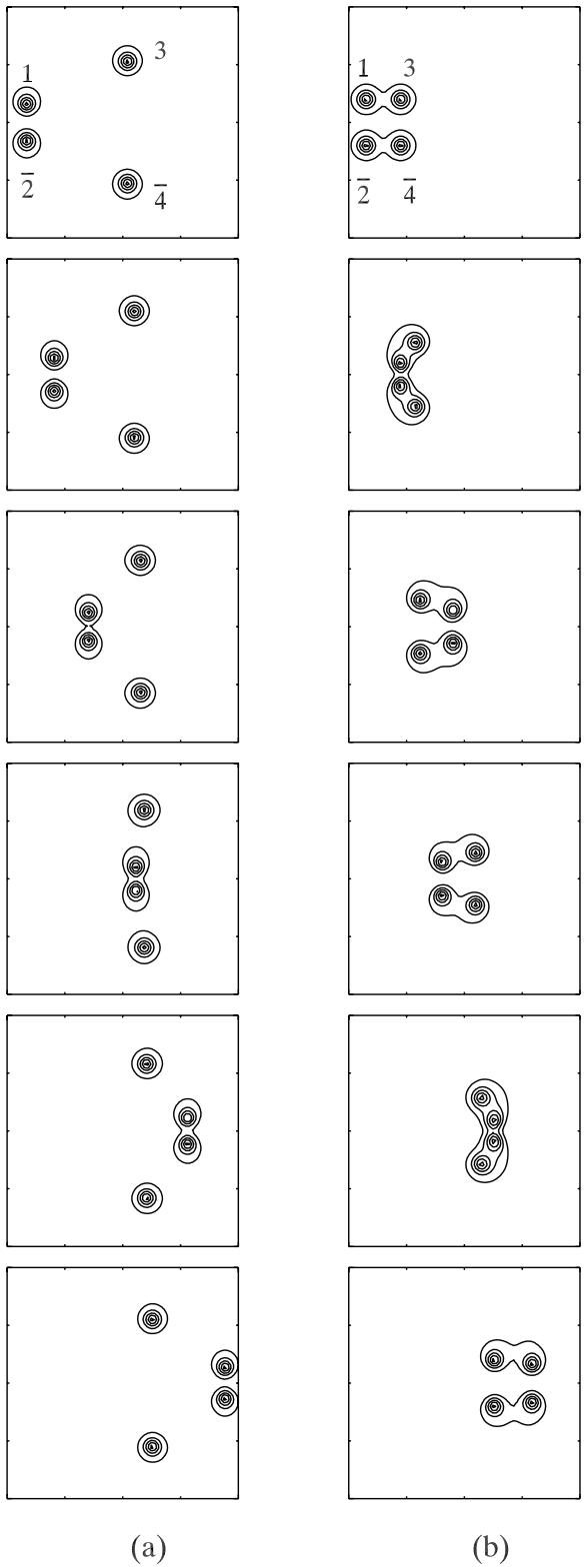

Fig. 3. Head-tail collisions between vortex-antivortex pairs. We plot here contours of the third component of the spin using the levels 0.1, 0.3, 0.5, 0.7, 0.9. The numbers 1, 3 denote the vortices and the $\overline{2}$, $\overline{4}$ the antivortices. In (a) the momentum difference is large and the pairs pass through each other. In (b) we have a propagating quadrupole state. The boxes have dimensions 40×40, the simulations were done in a space 100×100.

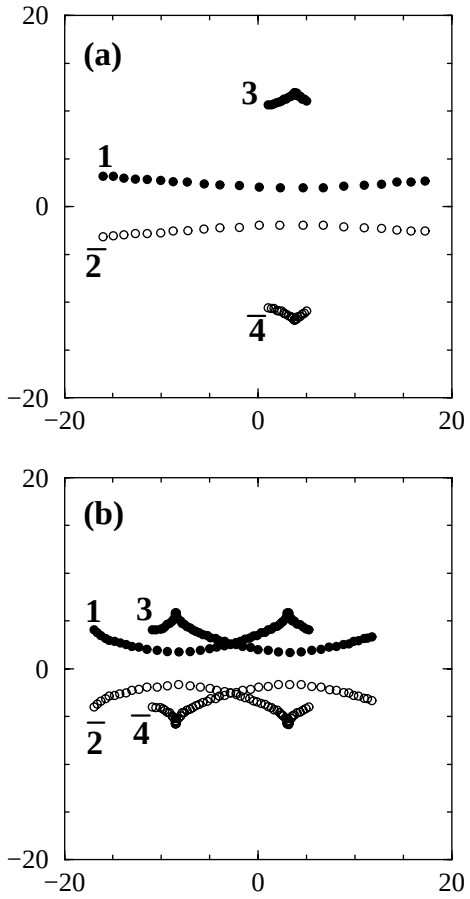

Fig. 4. The orbits of the vortices and antivortices of Figure 3 during their head-tail collision. The filled circles denote the position of vortices and the open circles the position of the antivortices at successive and equal times intervals. The numbers $1, \overline{2}, 3, \overline{4}$ denote the initial position of the vortices and antivortices.

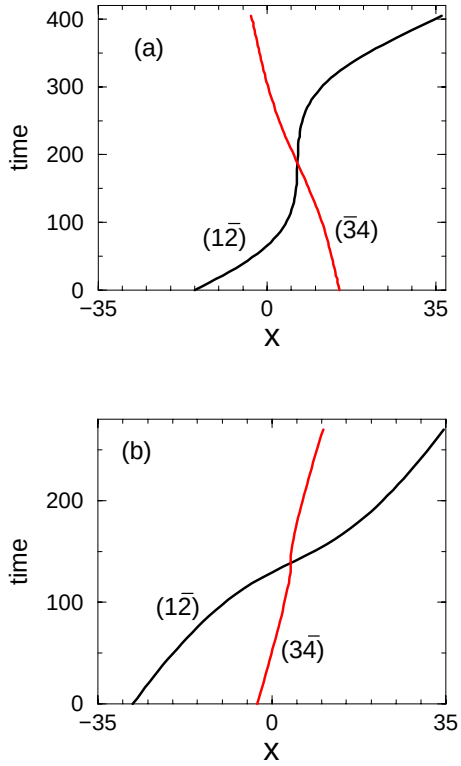

Fig. 5. (a) shows the positions on the x-axis of the two pairs $(1\overline{2})$ and $(\overline{3}4)$ as a function of time, for the simulation of Figures 1c. (b) shows the positions on the x-axis of the two pairs $(1\overline{2})$ and $(3\overline{4})$ as a function of time, for the simulation of Figures 3a. See text for details.

of a large difference (Figs. 1c and 2c). In the latter case one expects that the vortices which belong to different pairs will interact loosely with the vortices of the other pair. As a result, the two pairs are expected to travel almost undistracted. We use the ansatz (16) with the parameters $L_1 = 4,\ L_2 = 7L_1 = 28$. The initial separation of the pairs is $\delta = 30$. The result is close to expectations, that is the small pair passes through the large one. The distortion in the trajectories should become smaller as the size of the large pair becomes larger. This case is thus analogous to soliton interaction in one-dimensional integrable systems, as has been noted by Aref [27].

In order to explore further this analogy we have plotted in Figure 5a the x-coordinate of the two pairs as a function of time. (The data of Fig. 2c correspond to the data of Figure 5a only until time = 345.) We observe that the fast pair experiences a delay during the interaction with the slow one, which results in a negative shift (in comparison to the free motion) in its x-position after the collision. On the other hand, the slow pair is accelerated during the interaction and thus gains a positive shift in its x-position. The present observation should be contrasted to the situation in one-dimensional soliton collisions where a positive shift for both solitons is observed in all models.

An intermediate situation between those in Figures 1a and 1c is presented in Figure 1b. The parameters in the initial ansatz are $L_1 = 4,\ L_2 = 6L_1 = 24,\ \delta = 34$. The pairs initially exchange partners during the scattering process and form new V-A pairs just as in the simulation in Figure 1a. However, after some excursion the new pairs approach each other again, exchange partners once more and the initial pairs re-emerge traveling along their initial direction of motion. The trajectories followed by the vortices are depicted in Figure 2b. A similar scenario for point vortices in hydrodynamics has been discussed in [28].

In the next set of simulations we explore the situation of a head-tail collision. That is, both the slow and the fast pair move to the same direction (to the right in Figs. 3a, 4a). The parameters here are $L_1 = 8,\ L_2 = 20,\ \delta = 25$. The two pairs pass through each other, but some difference to the case of Figure 1c should be pointed out. In Figure 5b we give the x-component of the trajectories of the pairs. We find that the fast pair is accelerated during the interaction (positive shift) while the slow pair is decelerated (negative shift). (See, however, the relevant remarks in the next section.)

The last simulation, presented in Figures 3b and 4b, includes two identical V-A pairs traveling along the same direction. It can be considered as a limiting case to that

of Figure 3a when the sizes of the pairs are equal. The parameter values are $L_1 = 8,\ L_2 = 8,\ \delta = 6$. The system can be also viewed as a vortex-vortex pair and an antivortex-antivortex pair. Both pairs rotate while at the same time the magnetic quadrupole which is formed is propagating along the x-axis. A similar "leap-frogging" motion was studied in hydrodynamics by Love [29] and has also been observed with two vortex rings [30]. Since the magnetic quadrupole is characterized by two parameters (the velocity and the internal frequency) it can be considered as an analog of a breather [27,28]. We can make an estimate of the mean velocity of propagation of the quadrupole. Suppose that L is the mean distance of the pair of vortices from the pair of antivortices. If this is large compared to the distance between vortices of the same kind we may consider the quadrupole as two dipoles on top of each other. Then, a straightforward generalization of the results of [9] gives

$$v \simeq \frac{2}{L}, \qquad L \gg 1. \tag{17}$$

The rough estimate says that the quadrupole propagates with twice the velocity of a single V-A pair. In the present case, we have $L = 8$ which implies a velocity $v \simeq 0.25$. Indeed, our simulations show that the quadrupole in Figures 3b, 4b, propagates with a mean velocity $v_q \simeq 0.24$ while a single V-A pair with a size $L = L_1 = 8$ has a mean velocity $v_d \simeq 0.125$.

The richness of the above results shows that exploring numerically the different scenarios that occur during the interaction of two V-A pairs is a rather cumbersome task. We note that in the processes that we have been studying all the vortices retain their identity during collision. This implies that an analytical calculation based on collective coordinates should be successful in reproducing the numerical results and should also provide an overview of the observed phenomena. This task will be taken up in the next section.

In the remainder of the present section we continue with simulations of collisions of solitons which do not have a distinct vortex-antivortex pair character. We use here again the semitopological solitons found in [9]. An example is given in Figure 6. In the initial state, in the first entry of the figure, the V-A pair on the right has a velocity $v_2 = 0.1$ while the other soliton on the left has a large velocity, specifically here $v_1 = 0.9$, and has no vortex-antivortex character. The clear numerical result, shown in the remaining five entries of the figure, is that the fast soliton is split at collision time in a vortex and an antivortex. The outcome is two identical V-A pairs which are scattered at an angle.

We perform a series of simulations of collisions between solitons, where one of them has a definite velocity – we chose $v_2 = 0.1$ – while the velocity of the other one varies in the range $0.1 \leq v_1 < 1$. The results are summarized in Figure 7 which gives the cosine of the scattering angle θ as a function of the velocity v_1 of the fast soliton (filled circles connected with a solid line in the figure). The scattering angle is measured (in Fig. 6) from the negative horizontal

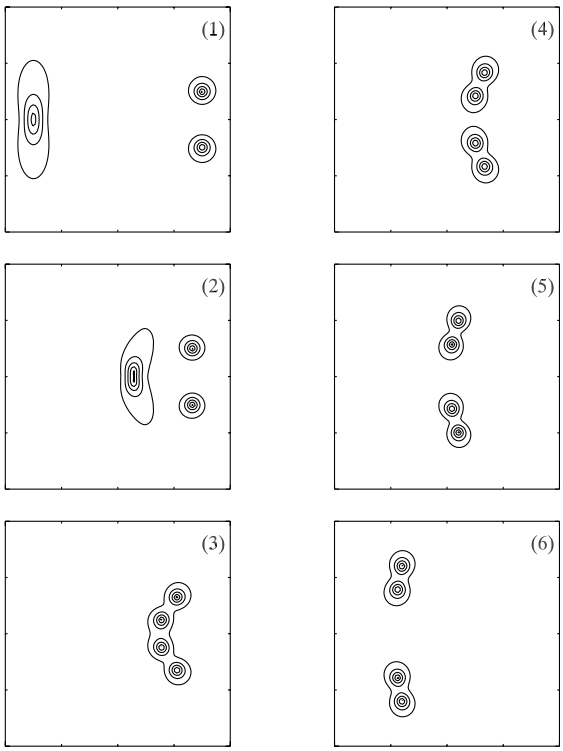

Fig. 6. Head-on collision between a slow V-A pair with velocity $v_2 = 0.1$ (right in the first entry) and a fast soliton with velocity $v_1 = 0.9$ (left in the first entry). We present six snapshots at times $t = 0$, 22, 44, 66, 88, 132. The fast soliton is split in a vortex and an antivortex at the time of collision. The vortices exchange partners and two new pairs are formed which are scattered at an angle.

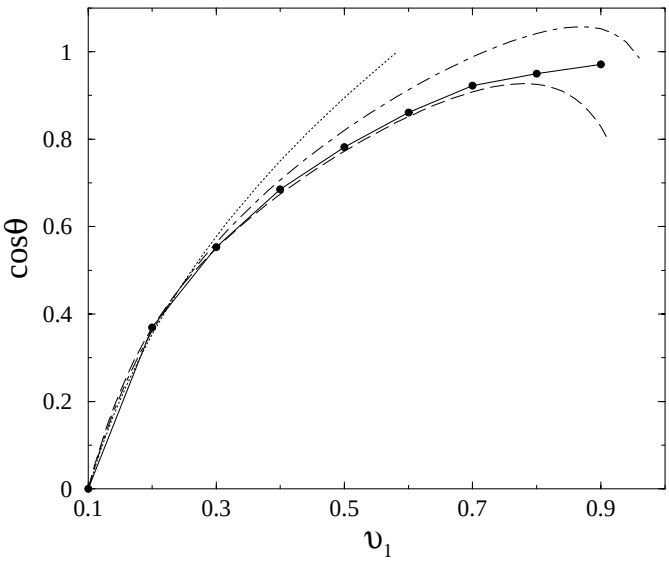

Fig. 7. The cosine of the scattering angle for a series of simulations where the slow soliton has a velocity $v_2 = 0.1$ and the fast one $0.1 \leq v_1 < 1$, is given by the dots which have been connected by a solid line. The dashed line results from conservation of energy and linear momentum. The dotted and the dot-dashed lines give the result of formula (35) for two different methods of calculating the soliton lengths (see text for details).

axis. We have $\theta = \pi/2$ when the velocities of the two solitons are equal, that is when $v_1 = v_2 = 0.1$. It is then monotonically decreasing as v_1 increases until the value $v_1 \simeq 0.9$.

When the velocity of the second soliton becomes greater than the value $v_1 \simeq 0.91$ we face a new scenario. The soliton is initially split into a V-A pair, then follows a loop and finally it re-joins its initial partner. We eventually obtain the picture of two solitons which have passed through each other. The scenario resembles that of Figure 1b. The difference here is that, well after the collision time, the fast soliton is destabilized. When the velocity of the fast soliton is increased, the loop that the vortices follow during collision becomes smaller. For $v_1 \gtrsim 0.97$ we have no loop any more, and the fast soliton passes through the slow pair.

The value $v_2 = 0.1$ used in the simulations in Figure 7 is not special. We can obtain results similar to those in Figure 7 using a different v_2, *e.g.* $v_2 = 0.2$ or 0.3. The value of v_1 until which scattering at an angle occurs, seems to be close to the value $v_1 = 0.9$ in these cases, too. For increasing v_2 the minimum scattering angle, that we can obtain by simulations, increases.

The simulations of this section give an overview of the possible scattering scenarios. However, the picture will not be complete until we obtain an analytical understanding. The theory which we present in the next section accounts for the simulations presented in Figures 1, 3 and provides a reasonably satisfactory understanding. A step towards the understanding of the results of Figures 6, 7 will also be taken.

4 Collision of vortex-antivortex pairs: analytical description

A full analytical investigation of interactions between vortex pairs appears to be quite complicated. Suffice it to say that no analytical formula is known for a single vortex pair soliton. However, one can employ a rigid shape approximation and suppose that each vortex is a coherently traveling structure and is also well separated from all the others. Then the dynamics of the system of vortices reduces to that of their centers $\mathbf{R}_i$. The latter obey the equations [20,4]

$$\frac{\mathrm{d}\mathbf{R}_i}{\mathrm{d}t} \times \mathbf{G}_i = \mathbf{F}_i, \tag{18}$$

where $\mathbf{G}_i$ is the gyrocoupling vector (11) for vortex i and $\mathbf{F}_i \equiv -\partial E/\partial \mathbf{R}_i$. The quantity E is the interaction energy between the vortices, therefore we call $\mathbf{F}_i$ the force on vortex i exerted by the other vortices in the system.

To make further progress we need the form of E, that is we need to know the field of the vortices. Under the assumption that the vortices are "quasi-static" the field of a single vortex is approximately given by equations (12, 13). One should note that the energy is finite only when

$$\sum_i \kappa_i = 0, \tag{19}$$

where κ_i is the vortex number of a single vortex. We shall study only this situation here. Then the energy E of the vortex interaction has the form [31]

$$E \simeq -2\pi \sum_{i<j} \kappa_i \, \kappa_j \, \ln(|\mathbf{R}_i - \mathbf{R}_j|), \tag{20}$$

where a constant has been omitted.

We put $\mathbf{R}_i = (X_i, Y_i)$ in equation (18) and obtain

$$\frac{\mathrm{d}X_i}{\mathrm{d}t} = -\sum_{j\neq i} \kappa_j \, \frac{(Y_i - Y_j)}{(\mathbf{R}_i - \mathbf{R}_j)^2},$$

$$\frac{\mathrm{d}Y_i}{\mathrm{d}t} = \sum_{j\neq i} \kappa_j \, \frac{(X_i - X_j)}{(\mathbf{R}_i - \mathbf{R}_j)^2}. \tag{21}$$

These are the same as the equations of motion of point vortices in hydrodynamics [15,16] when the hydrodynamic "vortex strengths", which correspond to κ_i in the present system, are ± 1.

One can now see that

$$P_x = \sum_i P_i^x = \sum_i 2\pi \, \kappa_i \, Y_i,$$

$$P_y = \sum_i P_i^y = -\sum_i 2\pi \, \kappa_i \, X_i, \tag{22}$$

as well as

$$\ell = \sum_i 2\pi \, \kappa_i \, (X_i^2 + Y_i^2) \tag{23}$$

are conserved quantities. Equations (22) give the two components of the total momentum and equation (23) gives the total angular momentum of the system. They can be derived from the formulas (9, 10) when the rigid-shape approximation is used. We further note that equations (18) can be derived as the Hamilton equations associated with the Hamiltonian (20) with the conjugate variables X_i and $P_i^x = 2\pi \, \kappa_i \, Y_i$.

In general, system (21) is integrable only for a system of three point vortices. However, for a system of two V-A pairs, for which condition (19) is satisfied, equations (21) can be integrated, when the pairs are initially moving along the same line [32]. This is a fortunate situation since we shall be exclusively concerned with such systems in the present paper.

The approximations employed so far seem to be quite crude. For instance we expect the rigid-shape approximation to be valid when the distances between the vortices are much larger than the size of the out-of-plane structure of each vortex (unity in our units). This could severely restrict the applicability of equations (21). However, the numerical simulations, of the previous section, indicate that the results of the present approximate theory could be qualitative correct even for situations beyond the applicability limits of the theory.

In the following we give the equations of motion of two V-A pairs. The vortex and antivortex of the first pair

are placed at positions $(x_1, \pm y_1)$ and have $\kappa = \pm 1$. We denote this pair schematically as $(1\overline{2})$. The second pair is at $(x_2, \pm y_2)$, has $\kappa = \mp 1$, and is denoted $(\overline{3}4)$. (*cf.* top entries of Fig. 1.) We choose the polarity $\lambda = 1$ for all vortices. The system represents two V-A pairs in a head-on collision course. From equations (21) we derive the four equations of motion

$$\frac{\mathrm{d}x_1}{\mathrm{d}t} = \frac{1}{2y_1} + \frac{y_1 - y_2}{(x_1 - x_2)^2 + (y_1 - y_2)^2} - \frac{y_1 + y_2}{(x_1 - x_2)^2 + (y_1 + y_2)^2}, \tag{24}$$

$$\frac{\mathrm{d}y_1}{\mathrm{d}t} = -\frac{x_1 - x_2}{(x_1 - x_2)^2 + (y_1 - y_2)^2} + \frac{x_1 - x_2}{(x_1 - x_2)^2 + (y_1 + y_2)^2}, \tag{25}$$

$$\frac{\mathrm{d}x_2}{\mathrm{d}t} = -\frac{1}{2y_2} + \frac{y_1 - y_2}{(x_1 - x_2)^2 + (y_1 - y_2)^2} + \frac{y_1 + y_2}{(x_1 - x_2)^2 + (y_1 + y_2)^2}, \tag{26}$$

$$\frac{\mathrm{d}y_2}{\mathrm{d}t} = -\frac{x_1 - x_2}{(x_1 - x_2)^2 + (y_1 - y_2)^2} + \frac{x_1 - x_2}{(x_1 - x_2)^2 + (y_1 + y_2)^2}. \tag{27}$$

The system (24–27) is completely integrable since there are four independent conserved quantities. We shall use the energy and the x-component of the linear momentum:

$$y_1 y_2 \frac{(x_1 - x_2)^2 + (y_1 - y_2)^2}{(x_1 - x_2)^2 + (y_1 + y_2)^2} = y_1^{(0)} y_2^{(0)}, \tag{28}$$

$$y_1 - y_2 = y_1^{(0)} - y_2^{(0)}. \tag{29}$$

We suppose that the pairs are initially on the x-axis and at an infinite distance from each other. Then, $y_1^{(0)}, y_2^{(0)}$ denote the y-coordinates of the vortices at time $t = -\infty$.

We define $L_1 \equiv 2y_1^{(0)}$ and $L_2 \equiv 2y_2^{(0)}$ as the sizes of the pairs. We take $L_2 \geq L_1$ while $L_1, L_2 \gg 1$. Therefore we have for the velocities:

$$v_1 = \frac{1}{L_1}, \qquad v_2 = \frac{1}{L_2}, \tag{30}$$

that is, $(1\overline{2})$ is the "small" and fast pair and $(\overline{3}4)$ is the "large" and slower pair. Equations (24–27) were studied within the framework of hydrodynamics in [28,29,33]. It was shown that the behavior of the pairs during scattering depends on the ratio $\alpha = L_2/L_1 = v_1/v_2$. There are the following three cases:

(a) when $1 \leq \alpha < \alpha_1 = 3 + 2\sqrt{2} \simeq 5.83$, the pairs change partners during the process and scatter at an angle (Fig. 1a).

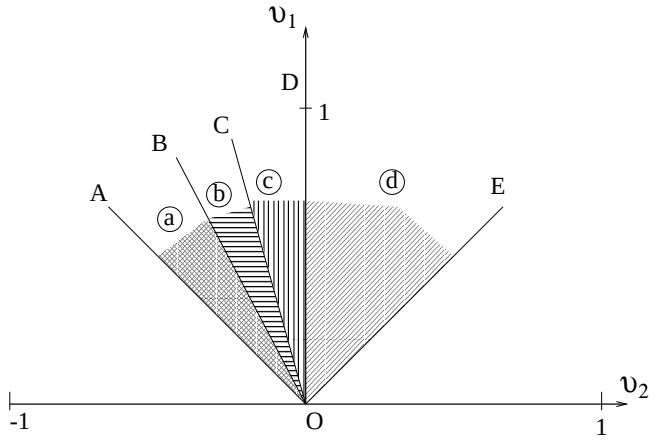

Fig. 8. A schematic overview of the different possibilities for head-on and head-tail collision between two soliton pairs. v_1 and v_2 are the velocities of the two pairs. The regions a, b and c correspond to to the cases a, b and c of Figure 1. The region d corresponds to the case of Figure 3a and the scenario of Figure 3b occurs for velocities on the line OE.

(b) In the intermediate case, when $\alpha_1 < \alpha < \alpha_2 = (\sqrt{2} + \sqrt{\sqrt{5} - 1})/(\sqrt{2} - \sqrt{\sqrt{5} - 1}) \simeq 8.35$, the vortices change partners during scattering but later they rejoin their initial partners and travel along the initial direction of motion (Fig. 1b).

(c) When $\alpha > \alpha_2$ the fast pair passes through the slow one (Fig. 1c).

In Figure 8 we give a schematic representation of the different regions in the (v_1, v_2) plane where the three scattering processes occur.

In case (a) the scattering process can be described by $(1\overline{2}) + (\overline{3}4) \rightarrow (1\overline{3}) + (\overline{2}4)$ which is a schematic representation of the change of partners during collision. In the limit of two identical pairs one can use Love's [29] equation (28) to obtain the following well-known result

$$\frac{1}{x_1^2} + \frac{1}{y_1^2} = \frac{1}{\left(y_1^{(0)}\right)^2}, \tag{31}$$

which is in good agreement with the data of the numerical simulation of the Landau-Lifshitz equation [24]. In the general case of two different ingoing pairs, the outgoing pairs will actually be identical. Equations (28, 29) give for the size of the two identical outgoing pairs

$$L_{\mathrm{out}} = \sqrt{L_1 L_2}. \tag{32}$$

This formula is known for point-like vortices in 2D hydrodynamics of incompressible fluids [16].

The angle of scattering can be found if we use the laws of conservation of energy and linear momentum:

$$E = \frac{E_1 + E_2}{2}, \qquad P \cos\theta = \frac{P_2 - P_1}{2}, \tag{33}$$

where E is the energy and P the absolute value of the linear momentum on the x-axis of each of the final pairs.

The angle θ is measured from the direction of motion of the slow pair. We obtain

$$\cos\theta = \frac{P_2 - P_1}{2P} \cdot \tag{34}$$

The calculation of P requires the use of the energy conservation law and the energy-momentum dispersion relation which is known numerically [9].

Figure 7 shows the numerical results (filled circles connected by lines) for the $\cos\theta$ as a function of v_1, keeping a constant $v_2 = 0.1$. We have $v_1 > v_2$. The dashed line results from equation (34) and it is a very good approximation of the simulation results until $v_1 \sim 0.78$. At this value the dashed line has a maximum. Until this critical value of v_1 the collision is elastic in the sense that almost no energy is dissipated in radiation. We also have to mention that the approximation shown by the dashed line is getting worse as the velocity v_2 is increasing.

In the approximation of equations (24–27) and (30) we have for the scattering angle:

$$\cos\theta = \frac{\alpha - 1}{2\sqrt{\alpha}} \cdot \tag{35}$$

The limiting cases are $\theta = \pi/2$ for $\alpha = 1$ and $\theta = \pi$ when $\alpha = \alpha_1$. Some care is needed in interpreting the angle $\theta = \pi$ in the last limiting case. In this case the new pairs which emerge follow the parabolic orbit

$$x_1 = -\frac{2\,y_1^2}{L_2 - L_1} = -\frac{y_1^2}{2(1+\sqrt{2})\,y_1^{(0)}} \cdot \tag{36}$$

The above results, should be a good approximation in the limit of large L_1, L_2.

There is a simple way to apply equation (35) when the two colliding V-A pairs are slow and the vortex and antivortex in a pair are well separated. The size of each pair can be taken to be the distance between the two points where the spin variable reaches the north pole and its velocity is the inverse of it. This method gives fairly good results for simulations with pairs of the size used in Figure 1.

A comparison of equation (35) with numerical results is given in Figure 7. The cosine of the angle θ for $1 \leq \alpha \leq \alpha_1$, is plotted by a dotted line. Figure 7 shows $\cos\theta$ as a function of v_1, for $v_2 = 0.1$. (not as a function of α). We have $v_1 > v_2$ and we consider $\alpha = v_1/v_2$. The dotted line is a poor approximation to the simulation results for $\alpha > 4$ ($v_2 > 0.4$). The deviation from the numerical points is even qualitatively wrong already for $v_2 \gtrsim 0.583$.

We recall at this point that in our simulations of the previous section we obtained results which could be understood as interaction processes between two dipoles even in the cases where the V-A pairs have no apparent dipole character. Exploiting this remark we assume that the V-A pair solitons (even those with large velocities and no apparent vortex-antivortex character) are dipoles with a length L and a charge q. To be sure, in the limit that the velocity goes to zero, L should go to the simple definition of length described in the previous paragraphs and q should go to the vortex number $\kappa = \pm 1$. In general, however, we use a generalization of equations (22, 15) and write for the momentum and velocity of such a dipole:

$$P = 2\pi\, qL, \qquad v = \frac{q}{L} \cdot \tag{37}$$

The length and charge of the dipole are then given by

$$L = \sqrt{\frac{P}{2\pi v}}, \qquad q = \sqrt{\frac{Pv}{2\pi}}, \tag{38}$$

where the values for P, v can now be taken from the Table of reference [9]. In the limit $v \to 0$ we use the relation $Pv = 2\pi$ to find that $L = 1/v \to \infty$ and $q = \pm 1$, which is the expected limit. In the opposite limit $v \to 1$, an asymptotic analysis [9] gives that $P \sim 1/\sqrt{1-v^2} \to \infty$, that is an infinite length of the dipole and also $q \sim 1/\sqrt{1-v^2} \to \infty$. For intermediate velocities the length L is finite and it reaches a minimum for $v \simeq 0.87$. The values for the charge q are relatively close to unity for $v < 0.5$ and they increase rapidly for $v > 0.9$.

The interesting result is presented in Figure 7 by the dot-dashed line. It is obtained by applying equation (35), where for α we substitute the ratio of lengths of the two V-A pairs given from equation (38). The curve is compared quite good with the results of the simulations even for large velocities. However, after $v_2 = 0.9$ the present approach fails completely. Indeed, we have no reason to believe that an approximation based on dipoles would be correct in the limit $v \to 1$.

We now turn to case (c) where the initial pairs survive throughout the process. For α large enough an expansion gives, with an error $\mathcal{O}(1/\alpha^4)$, the trajectories

$$\begin{aligned}
x_1 &= v_1\, t - \frac{4}{v_1} \arctan\left(2v_1 v_2\, t\right), \\
x_2 &= -v_2\, t - \frac{1}{\alpha^2}\,\frac{2}{v_2}\,\frac{(2v_1v_2t)}{1+(2v_1v_2t)^2} \\
&\quad -\frac{1}{\alpha^3}\,\frac{4}{v_2} \arctan(2v_1v_2t) + ... \\
y_1 &= y_1^{(0)}\left(1 + \frac{1}{\alpha}\,\frac{4}{1+(2v_1v_2\,t)^2}\right), \\
y_2 &= y_2^{(0)}\left(1 + \frac{1}{\alpha^2}\,\frac{4}{1+(2v_1v_2\,t)^2}\right),
\end{aligned} \tag{39}$$

where v_1, v_2 are given in equation (30) and the dots in the second equation stand for a lengthy term of order $1/\alpha^3$ which we shall not need in our analysis. It follows that, in this approximation, the fast pair $(1\overline{2})$ deviates strongly from the rectilinear motion. The shifts in the positions of the vortex pairs as time varies from $-\infty$ to ∞, are $\Delta x_1 = -4\pi/v_1$ for the fast pair and $\Delta x_2 = 4\pi/v_2\alpha^3$ for the slow one. (The terms in the dots do not give any shift in the pair position when times goes from $-\infty$ to ∞.) The shifts are measured relative to the direction of motion of each pair. The results of the simulations for the vortex system show that the fast pair is decelerated during the

collision as if it is repelled by the slow one, in agreement with equation (39). The simulations further show that the slow pair is accelerated during the collision as if it is attracted by the fast one. The final result is a positive and negative shift in the positions of the fast and slow pair, respectively, a phenomenon which has not been observed in head-on soliton collisions in one dimension. The obtained trajectories are similar to those for the 2D Euler equation [34].

In case (b), $\alpha_1 < \alpha < \alpha_2$, the scattering process is represented by the scheme $(1\overline{2}) + (\overline{3}4) \to (1\overline{3}) + (\overline{2}4) \to (1\overline{2}) + (\overline{3}4)$. This means that the vortices exchange partners at a first stage of the scattering, then the new pairs follow a looping orbit and at the final stage the initial partners rejoin and travel along the initial direction of motion (*cf.* Figs. 1c, 2c). The loop becomes the parabola (36) in the limit $\alpha = \alpha_1$ and it is a cusp when $\alpha = \alpha_2$.

We now turn to the head-tail collision. It corresponds to the area denoted (d) in Figure 8 and the relevant numerical simulations have been given in Figures 3 and 4. The case has been studied within a hydrodynamical context in [25,29,28]. As Love showed, only a slip-through motion (Fig. 3a) and a leap-frogging motion (Fig. 3b) can occur.

Suppose that vortices 1 and 3 have $\kappa = 1$ while $\overline{2}$ and $\overline{4}$ are antivortices and have $\kappa = -1$ (*cf.* Fig. 3a). The equations of motion are modified as follows: the left hand side of (24, 25) and the first term on the right hand side of (26) change their signs. The conserved quantities (28, 29) now read

$$y_1 y_2 \, \frac{(x_1 - x_2)^2 + (y_1 + y_2)^2}{(x_1 - x_2)^2 + (y_1 - y_2)^2} = y_1^{(0)} y_2^{(0)} \, \frac{\left(x_1^{(0)} - x_2^{(0)}\right)^2 + \left(y_1^{(0)} + y_2^{(0)}\right)^2}{\left(x_1^{(0)} - x_2^{(0)}\right)^2 + \left(y_1^{(0)} - y_2^{(0)}\right)^2}, \quad (40)$$

$$y_1 + y_2 = y_1^{(0)} + y_2^{(0)}. \quad (41)$$

The pairs are initially at $(x_1^{(0)}, \pm y_1^{(0)})$ and $(x_2^{(0)}, \pm y_2^{(0)})$. Using the above one can find that two pairs which start infinitely far apart will pass through each other for any value of $y_1^{(0)} < y_2^{(0)}$.

For a large difference in the size of the pairs ($\alpha \gg 1$) we find, by an expansion, the solution of the equations of motion (with an error $\mathcal{O}\left(\frac{1}{\alpha^4}\right)$):

$$\begin{aligned} x_1 &= v_1 t + \frac{4}{v_1} \arctan(2 v_1 v_2 t), \\ x_2 &= v_2 t - \frac{1}{\alpha^2} \frac{2}{v_2} \frac{(2 v_1 v_2 t)}{1 + (2 v_1 v_2 t)^2} \\ &\quad + \frac{1}{\alpha^3} \frac{4}{v_2} \arctan(2 v_1 v_2 t) + \ldots, \\ y_1 &= y_1^{(0)} \left(1 - \frac{1}{\alpha} \frac{4}{1 + (2 v_1 v_2 t)^2}\right), \\ y_2 &= y_2^{(0)} \left(1 + \frac{1}{\alpha^2} \frac{4}{1 + (2 v_1 v_2 t)^2}\right). \end{aligned} \quad (42)$$

The dots stand for terms of order $\mathcal{O}\left(\frac{1}{\alpha^3}\right)$ which do not contribute to the shift in the position of the pair when times varies from $-\infty$ to ∞. In the present case, the shift of the fast pair is to the direction of its motion $\Delta x_1 \simeq 4\pi/v_1$. The shift of the slow pair is also positive but small $\Delta x_2 \simeq 4\pi/(v_2 \alpha^3)$. However, the numerical simulations of the previous section (Fig. 5b) have given a small shift for the slow pair opposite to its direction of motion. We believe that this should be a consequence of the second term in the second of equations (42) which is dominant because of our small space and short integration time. We note here again a difference of the present system with the situation in 1D. For instance, in KdV the fast soliton acquires a positive shift and the slow one a negative shift due to a head-tail collision.

A difference between the head-on and head-tail collision for the case of large α, is that during the collision the size of the small pair increases in the head-on collision case (Eq. (39) and Fig. 1c) but it decreases in the head-tail collision case (Eq. (42) and Fig. 3a).

In the limit of a small difference of the sizes of the pairs ($\alpha \simeq 1$) the relative shift of the pairs grows and tends to infinity for identical pairs like $\Delta x_1 - \Delta x_2 \sim 4/(v_1 - v_2)$. In the limit of two identical pairs the asymptotes of the solution after the scattering have the form $x_2 = Vt - \sqrt{t}, x_1 = Vt + \sqrt{t}$ and, at large distances, the distance between pairs goes as $x_1 - x_2 = 2\sqrt{t}$. It is interesting to compare this shift with that for solitons in 1D systems where the shift is proportional to the logarithm of the difference of the velocities of the two solitons ($\Delta x_1 \sim \ln(v_1 - v_2)$) and the distance between two identical solitons after collision goes like $x_1 - x_2 \sim \ln t$.

Two V-A pairs which have a finite distance between them, will pass through each other when the following relation holds

$$\frac{\left(y_2^{(0)} + y_1^{(0)}\right)^2 \left[\left(y_2^{(0)} + y_1^{(0)}\right)^2 - 2\left(y_2^{(0)} - y_1^{(0)}\right)^2\right]}{\left(y_2^{(0)} - y_1^{(0)}\right)^2} > \left(x_2^{(0)} - x_1^{(0)}\right)^2. \quad (43)$$

In the opposite case, the pairs form a translating bound quadrupole state. The translation is accompanied by a rotation of the two vortices and the two antivortices around each other. This leap-frogging motion was first analyzed in [29]. An example is given in Figures 3b and 4b. The quadrupole state has lately acquired special interest due to its relation to breather modes [28].

We shall analyze some characteristics of the leap-frogging motion in the case that the two rotating vortices are well separated from the two rotating antivortices. We call L the distance between the two pairs. The two vortices rotate clockwise and the two antivortices counterclockwise. The translational motion of the quadrupole has the velocity given in equation (17). With the further assumption that the distance δ between the vortices of the

same pair is large compared to the size of a single vortex (but still small compared to the size of the quadrupole: $L, \delta \gg 1, L \gg \delta$), we find from equations (39) the frequency of rotation

$$\omega \simeq \frac{2}{\delta^2} - \frac{2}{L^2} \,. \tag{44}$$

5 Conclusions

We have presented a detailed study for the head-on and head-tail collisions between vortex-antivortex pairs in 2D easy-plane ferromagnets. The V-A pairs are the simplest units which can be found in free translational motion in our model. However, they have a nontrivial internal structure which is responsible for their unusual behavior during interaction. Our study combines numerical simulations, which yield a variety of interesting scattering scenarios, with a collective variable theory, which leads to an understanding of the main features of the scattering scenarios. The change of partners between V-A pairs during interaction is the most remarkable effect in our case. It is due to the internal structure of the V-A pairs which has been fully taken into account.

In a study of a system of a lot of vortices the mechanisms which have been described here should play a dominant role in the way to the final steady state. The relaxation process should include a multitude of collisions of vortices and the formation of steady structures.

From the point of view of soliton theory in two dimensions, our results are novel and can be compared with a variety of studies in the field. Some comparison is also done with soliton theory in one space dimension.

The scattering of coherently traveling objects in two dimensions appears to be of interest in a variety of physical systems. Objects similar to the V-A pairs studied here exist in systems in different fields of physics [12–15]. Even in nonequilibrium systems [35,36] studies similar to the present one have been performed and some similar results have been derived.

We thank H. Büttner for giving the initial stimulus for this work and for interesting conversations. We also thank the authors of [9] for kindly providing us the numerical code for the calculation of the V-A pair solitons. A.S.K. thanks the University of Bayreuth for its hospitality. A.S.K. and S.K. acknowledge financial support from the Graduiertenkolleg "Nichtlineare Spektroskopie und Dynamik".

References

1. A.S. Kovalev, A.M. Kosevich, K.V. Maslov, JETP Lett. **30**, 321 (1979).
2. A.M. Kosevich, V.P. Voronov, I.V. Manzhos, Sov. Phys. JETP **57**, 86 (1983).
3. A.V. Nikiforov, E.B. Sonin, Sov. Phys. JETP **58**, 373 (1983).
4. D.L. Huber, Phys. Rev. B **26**, 3758 (1982).
5. M.E. Gouvea, G.M. Wysin, A.R. Bishop, F.G. Mertens, Phys. Rev. B **39**, 11840 (1989).
6. F.G. Mertens, G.M. Wysin, A.R. Völkel, A.R. Bishop, M.J. Schnitzer, in *Nonlinear Coherent Structures in Physics and Biology*, edited by H.H. Spatschek, F.G. Mertens, NATO ASI Series, B; Vol. **329** (Plenum Press, New York and London, 1994).
7. F.G. Mertens, A.R. Bishop in *Nonlinear Science at the dawn of the 21st century*, edited by P.L. Christiansen, M.P. Soerensen, A.C. Scott, Springer Lecture Notes (Springer, Berlin, 2000).
8. N. Papanicolaou, T.N. Tomaras, Nuclear Physics B **360**, 425 (1991).
9. N. Papanicolaou, P.N. Spathis, Nonlinearity **12**, 285 (1999).
10. N.R. Cooper, Phys. Rev. Lett. **80**, 4554 (1998).
11. L.P. Pitaevskii, Sov. Phys. JETP **13**, 451 (1961).
12. C.A. Jones, P.H. Roberts, J. Phys. A **15**, 2599 (1982).
13. C.A. Jones, S.J. Putterman, P.H. Roberts, J. Phys. A **19**, 2991 (1986).
14. B. Luther-Davis, R. Powles, V. Tikhonenko, Opt. Lett. **19**, 1816 (1994).
15. H. Lamb, *Hydrodynamics* (Cambridge University Press, 1993).
16. H.J. Lugt, *Introduction to Vortex Theory* (Vortex Flow Press, Potomac, Maryland, 1996).
17. A.M. Kosevich, B.A. Ivanov, A.S. Kovalev, Phys. Rep. **194**, 117 (1990).
18. M.M. Bogdan, A.S. Kovalev, JETP Letters **31**, 424 (1980).
19. S. Komineas, N. Papanicolaou, Nonlinearity **11**, 265 (1998).
20. A.A. Thiele, Phys. Rev. Lett. **30**, 230 (1973).
21. A.R. Völkel, F.G. Mertens, A.R. Bishop, G.M. Wysin, Phys. Rev. B **43**, 5992 (1991).
22. A.R. Völkel, G.M. Wysin, F.G. Mertens, A.R. Bishop, H.J. Schnitzer, Phys. Rev. B **50**, 12711 (1994).
23. N. Papanicolaou, W.J. Zakrzewski, Physica D **80**, 225 (1995).
24. S. Komineas, Physica D **155**, 223 (2001).
25. W. Gröbli, *Specielle Probleme über die Bewegung geradliniger paralleler Wirbelfäden, Zürich, Zürcher und Furrer* (1877).
26. A.G. Greenhill, Q. J. Math. **15**, 10 (1878).
27. H. Aref, Ann. Rev. Fluid. Mech. **15**, 345 (1983).
28. B. Eckhardt, H. Aref, Phil. Trans. R. Soc. Lond. A **326**, 655 (1988).
29. A.E.H. Love, Proc. London Math. Soc. **25**, 185 (1894).
30. Y. Oshima, J. Phys. Soc. Jpn **45**, 660 (1978).
31. J.M. Kosterlitz, D.J. Thouless, J. Phys. C **6**, 1181 (1973).
32. B. Eckhardt, Phys. Fluids **31**, 2796 (1988).
33. E. Acton, J. Fluid Mech. **76**, 561 (1976).
34. E.A. Overman, N.J. Zabusky, J. Fluid. Mech. **125**, 187 (1982).
35. S. Komineas, F. Heilmann, L. Kramer, Phys. Rev. E **63**, 11103 (2001).
36. J. Fineberg, O. Lioubashevski, Physica A **249**, 10 (1998).